Biophysical Chemistry 141 (2009) 59–65

Contents lists available at ScienceDirect

Biophysical Chemistry

journal homepage: http://www.elsevier.com/locate/biophyschem

# Effect of quinone on the fluorescence decay dynamics of endogenous flavin bound to bacterial luciferase

Elena V. Vetrova [a,1], Nadezhda S. Kudryasheva [b], Kwan H. Cheng [a,*]

[a] Department of Physics, Texas Tech University, Lubbock, Texas 79409, USA
[b] Siberian Federal University, Krasnoyarsk, 660041, Russia

ARTICLE INFO

*Article history:*
Received 9 December 2008
Accepted 21 December 2008
Available online 7 January 2009

*Keywords:*
Time-resolved fluorescence decay
Bioluminescence enzyme
Enzyme/xenobiotic interactions
Rotational dynamics of enzyme substrate

ABSTRACT

The interaction of quinone with luciferase from *Photobacterium leiognathi* was studied based on the fluorescence decay measurements of the endogenous flavin bound to the enzyme. Homologous 1,4-quinones, 1,4-benzoquinone, methyl-1,4-benzoquinone, 2-methyl-5-isopropyl-1,4-benzoquine and 1,4-naphthoquinone, were investigated. In the absence of quinone, the fluorescence intensity and anisotropy decays of the endogenous flavin exhibited two intensity decay lifetimes (~1 and 5 ns) and two anisotropy decay lifetimes (~0.2 and 20 ns), suggesting a heterogeneous quenching and a rotational mobility microenvironment of the active site of the luciferase, respectively. In the presence of quinone, the intensity decay heterogeneity was largely maintained, whereas the fraction of the short anisotropy decay component and the averaged rotational rate of FMN increased with the increasing hydrophobicity of the quinone. We hypothesize that the hydrophobicity of the quinone plays a role in the non-specific inhibition mechanism of xenobiotic molecules in the bacterial bioluminescence system via altering the rotational mobility of the endogenous flavin in the luciferase.



## 1. Introduction

Biosensors based on the bioluminescence enzyme systems have shown great biotechnological promise for detecting trace toxins for homeland security and monitoring ecological pollution [1–6]. In order to improve the efficiency, specificity and sensitivity of these biosensors, an understanding of the inhibition mechanisms of the key bioluminescence enzymatic processes due to the non-specific interactions of various exogenous target compounds, or analytes, is required.

In general, the efficiency of enzyme inhibition by small organic molecules is associated with their chemical structure and physiochemical characteristics, such as charge, size, functional groups, aliphatic substituents and hydrophobicity [7]. Among those characteristics, the hydrophobicity of the molecule is of particular interest since many target analytes of the bioluminescence-based biosensors for monitoring ecological pollution are highly hydrophobic [7,8]. Quinone belongs to a class of small, hydrophobic, xenobiotic molecules that pose significant health hazard to living organisms and represent the major ecological and environmental pollutants in certain regions of the industrial nations [7–10]. The biophysical mechanism underlying the inhibition of the bioluminescence process of luciferase, a key enzyme for the construction of bioluminescence-based biosensors, by quinones of different levels of hydrophobicity is the major focus of this fluorescence study.

Bacterial luciferase catalyzes the bioluminescence reaction of marine bacteria [11]. The catalytic process involves the oxidation of an endogenous flavin molecule (riboflavin 5'-phosphate or flavinmononucleotide (FMN)) and fatty aldehyde by molecular oxygen that results in the formation of an electron-excited product and, finally, emitting light at 490 nm. The detailed biochemical mechanism and the stage of electron-excited state formation of this bioluminescence process remain speculative [11–14]. Luciferase is a heterodimeric protein made up of two α and β subunits with molecular weights of 40 and 37 kDa, respectively [15]. The α unit contains an active center which binds one FMN molecule and is largely responsible for the kinetics of the bioluminescence process, whereas the β subunit is essential for a high quantum yield reaction [15,16].

The environment and conformational dynamics of the phosphate group, as well as the isoalloxazine ring of the endogenous FMN bound to luciferase are important for the catalytic process of the bioluminescence system [17]. Although the binding characteristics between the oxidized or reduced form of FMN and the apo-luciferase have been investigated, the exact number of FMN molecules bound to luciferase remains uncertain [11,17,18]. Our previous work has established that the endogenous FMN bound to luciferase represents a useful, intrinsic fluorophore to study the conformation and dynamics of the FMN binding region of the enzyme, as well as the subtle interactions of the

* Corresponding author. Science 101, Department of Physics, P.O. Box 41051, Texas Tech University, Lubbock, Texas 79409-1051, USA. Tel.: +1 806 742 2992; fax: +1 806 742 1182.
*E-mail address:* vckhc@ttacs.ttu.edu (K.H. Cheng).
[1] Present Address: Institute of Biophysics, Akademgorodok, 660036 Krasnoyarsk, Russia.

0301-4622/$ – see front matter © 2008 Elsevier B.V. All rights reserved.
doi:10.1016/j.bpc.2008.12.012

enzyme with non-fluorescent exogenous compounds, such as quinones [19–22].

In this work, both the fluorescence intensity decay and anisotropy decay of endogenous FMN were measured in the absence and presence of a series of homologous 1,4-quinones of different levels of structural complexity and hydrophobicity. Biexponential intensity and anisotropy decay behavior, of endogenous FMN was detected in the absence and presence of quinone. The correlation between the hydrophobicity of the added quinone and the decay dynamics parameter of the endogenous FMN was also examined.

## 2. Materials and methods

### 2.1. Materials

Bacterial luciferase was isolated from *Photobacterium leiognathi*. Details of the luciferase isolation procedure are given elsewhere [23]. Lyophilized luciferase was stored at −20 °C before use. Fluorescent dye, Coumarin 338, was obtained from Eastman Kodak (Rochester, NY) and was used as a fluorescence decay standard. FMN, 1,4-benzoquinone (Q1), 2-methyl-1,4-benzoquinone (Q2) and 2-methyl-5-isopropyl-,4-benzoquinone (Q3) were obtained from Sigma (St. Louis, MO), and 1,4-naphthoquinone (Q4) from Acros Organics (Pittsburgh, PA).

### 2.2. Sample preparation

To prepare the protein solution, luciferase was thawed and subsequently dissolved in a 0.05 M phosphate water-buffer solution (pH 6.8) at a concentration of 52 μM at room temperature (RT). A stock solution of quinone was freshly prepared in 100% ethanol at RT. Immediately before the fluorescence measurement, quinone was added directly to the above protein solution followed by rapid votexing for several minutes. The concentration of quinone was fixed at 3.6 mM. The final concentration of ethanol in the sample was less than 3 mol%. This level of ethanol has no detectable effect on the catalytic function of the bacterial enzyme [8]. As a control, a free FMN solution (2 μM) was prepared by dissolving FMN directly into the same phosphate buffer.

### 2.3. Fluorescence measurements

Time-resolved fluorescence (TRF) measurements of the endogenous FMN bound to luciferase (with and without the addition of quinone) and the free FMN solution (control) were performed in the frequency-domain on a GREG 200 fluorometer (ISS, Inc. Champaign, IL) equipped with digital multifrequency cross-correlation phase and modulation acquisition electronics [24–26]. For the fluorescence intensity decay ($I$(t)) measurements, phase delay and demodulation values of the FMN fluorescence and that of a Coumarin 338 standard in ethanol (fluorescence lifetime = 3.54 ns) were collected as a function of the intensity-modulation frequency (1–150 MHz) of the excitation source. Here, a Liconix 4240 NB continuous wave He–Cd laser (Santa Clara, CA) emitting at 442 nm was used as the excitation source, and a 465 nm low-cutoff filter was employed to collect the fluorescence emission. An excitation polarizer with its transmission axis set at 35° and no emission polarizer on the emission channel were used to eliminate the rotational diffusion effect of the sample to the $I$(t) measurements [27]. For the fluorescence anisotropy decay ($r$(t)) measurements, differential polarized phase shift and polarized demodulation ratio were collected at the same modulation frequency range. Here, both excitation and emission polarizers were used. Details of the above TRF measurements have been described elsewhere [24–26,28–30]. Steady-state fluorescence spectral and anisotropy measurements were also performed using the GREG 200 fluorometer but using only the single-photon counting mode [26,30].

### 2.4. Fluorescence decay dynamics analysis

Multiexponential decay functions were used to analyze the $I$(t) and $r$(t) data of FMN as shown below.

$$I(t) = \sum_{i=1}^{N} \alpha_i e^{-t/\tau_i} \quad (1)$$

$$r(t) = \sum_{i=1}^{N} \beta_i e^{-t/\phi_i} \quad (2)$$

Here, $\tau_i$ and $\alpha_i$ are the fluorescence intensity decay lifetime and the molar fraction of the $i$th decay species, and $N$ the total number of decay components in the sample. Similarly, $\phi_i$ and $\beta_i$ represent the anisotropy decay lifetime and the molar fraction of the $i^{th}$ rotational species in the sample. The anisotropy decay lifetime is inversely proportional to the rotational rate of the fluorophore. For $I$(t), the intensity fraction $f_i$ of the $i^{th}$ component and the intensity-averaged lifetime $\tau_{ave}$ are also determined as given below.

$$f_i = \alpha_i \tau_i / \sum_{i=1}^{N} \alpha_i \tau_i \quad (3)$$

$$\tau_{ave} = \sum_{i=1}^{N} f_i \tau_i \quad (4)$$

A first-order rotational decay time ($\phi_p$) can also be estimated from the measured steady-state anisotropy ($r_{ss}$) and $\tau_{ave}$ of the fluorophore without the use of $r$(t) according to the Perrin model [28,30] given below.

$$\phi_p = \frac{\tau_{ave}}{r_0/r_{ss} - 1} \quad (5)$$

Here $r_0$ is the initial anisotropy at $t = 0$. The value of $\phi_p$ is inversely proportional to the averaged rotational rate of the fluorophore.

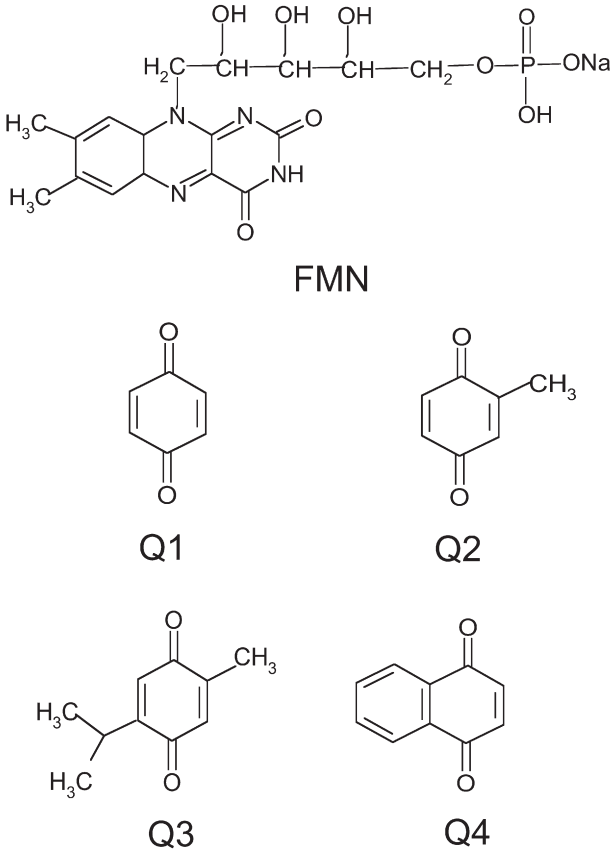


**Fig. 1.** Chemical structures of FMN and quinones, Q1, Q2, Q3 and Q4.

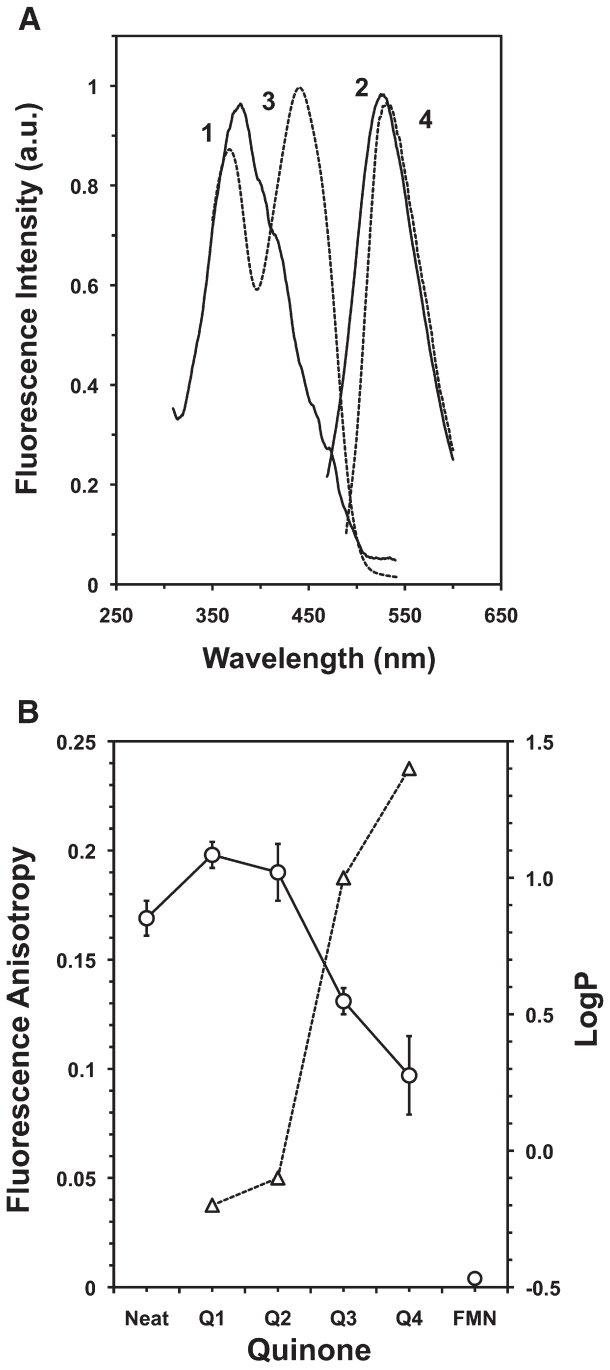


**Fig. 2.** Steady-state fluorescence characterization of the endogenous FMN. (Panel A) Excitation and emission spectra of the endogenous FMN bound in luciferase (1, 2) and that of the free FMN in solution (3, 4). (Panel B) Dependence of the fluorescence anisotropy of the endogenous FMN (circle) and partition coefficient, LogP, (triangle) with quinone (Q1–Q4). Anisotropy data from the neat, i.e., bound FMN in luciferase, and the free FMN in solution (control) are also shown. The uncertainties are indicated by bars.

The besting fitting of the frequency-domain data to the decay models above was based on the minimization of the reduced chisquare parameter using a nonlinear least square fitting algorithm [25].

## 3. Results

### 3.1. Structural and hydrophobic characteristics of quinone

The chemical structures of the four small quinones and the larger FMN molecule used in this study are displayed in Fig. 1. These quinones represent a series of homologous 1,4-benzoquinone starting from Q1 to Q4 as shown. Note that Q2 and Q3 are the aliphatic derivatives of 1,4-benzoquinone (Q1) that share a common structural unit of a single-ring structure, whereas Q4 has a two-ring structure. Therefore, the addition of the extra aliphatic groups in Q2 and Q3 and an extra ring in Q4 should render a progressive increase in the order of hydrophobicity of this quinone series. To confirm that, the values of the oil–water partition coefficient (Log P) of the quinones were obtained from PubChem, a public chemical database [31]. Here, Log P is defined as the logarithm of the ratio of concentration of the compound in octanol to that in water and, therefore, quantifies the level of hydrophobicity of the compound. As expected, a progressive increase in the value of LogP with the order of quinones from Q1 to Q4 was evident as shown in Fig. 2B.

### 3.2. Steady-state fluorescence measurements

Fig. 2A shows the fluorescence excitation and emission spectra of the endogenous FMN bound to the isolated bacterial luciferase and that of the free FMN in solution. For the free FMN (Fig. 1), two excitation peaks at ~375 and 450 nm, and a single emission peak at ~530 nm were obtained (Fig. 2A). For the endogenous FMN in luciferase, a similar emission peak but a single and slightly red-shifted excitation peak at ~400 nm, indicative of the semi-reduced form of the endogenous FMN [22], were observed. The values of the steady-state fluorescence anisotropy, i.e., $r_{ss}$, of the FMN bound to luciferase in the absence (neat) and presence of quinone (Q1 to Q4), as well as of the free FMN in solution are plotted in Fig. 2B. The value of $r_{ss}$ was ~0.17 in the neat sample, increased slightly to ~0.20 when Q1 or Q2 was added and declined sharply to ~0.13 and 0.10 in the presence of Q3 or Q4, respectively. For comparison, the value of $r_{ss}$ was ~0.004 for the free FMN in solution.

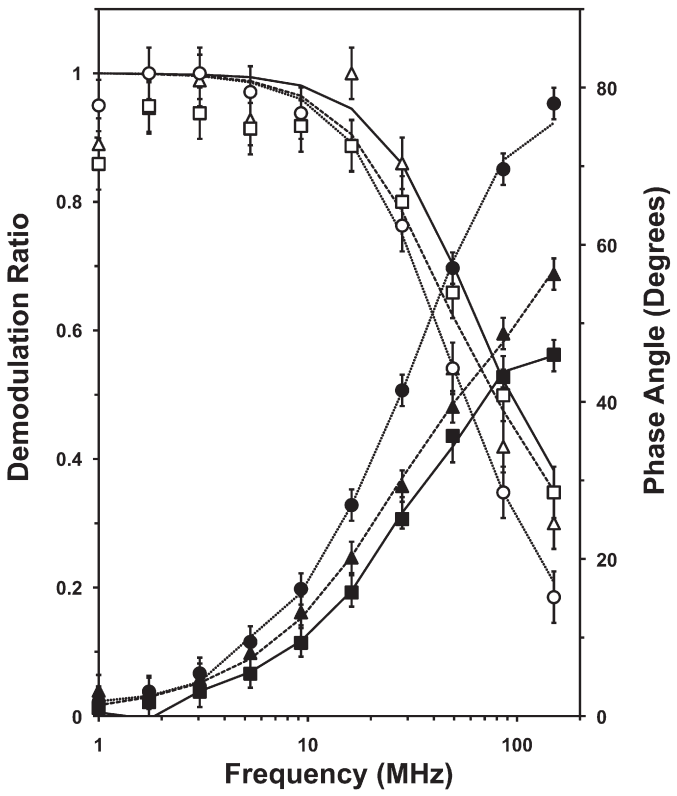


**Fig. 3.** Demonstration of the frequency-domain fluorescence intensity decay data of the free FMN in solution (circle), FMN in luciferase or neat (triangle) and luciferase in the presence of Q4 (square). The demodulation ratio (open symbols) and phase angle (solid symbols) are shown. The lines represent the biexponential decay fits to data for the neat and the luciferase in the presence of Q4, but a monoexponential decay for the free FMN. The uncertainties are indicated by bars.

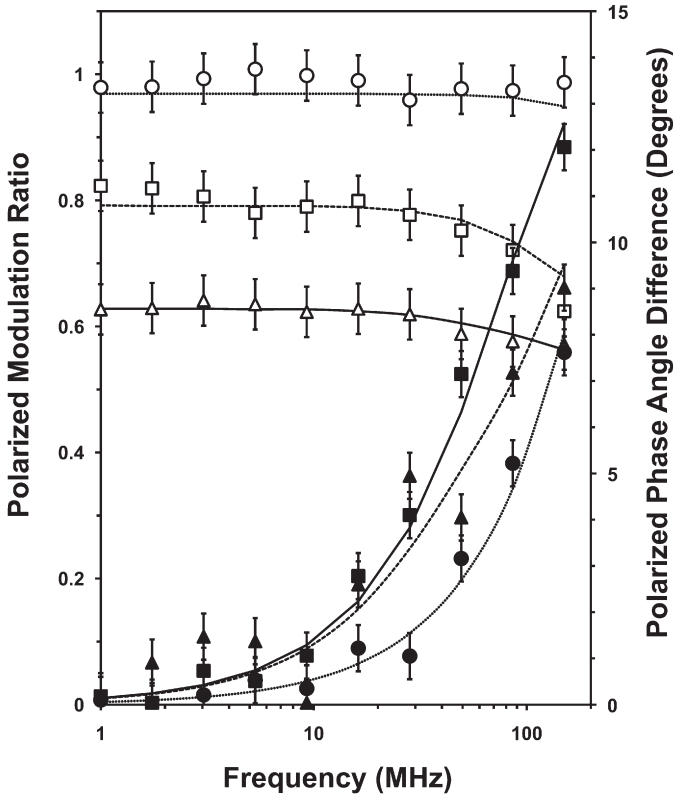


**Fig. 4.** Demonstration of the frequency-domain fluorescence anisotroy decay data of the free FMN in solution (circle), FMN in luciferase or neat (triangle) and luciferase in the presence of Q4 (square). The polarized modulation ratio (open symbols) and polarized phase angle difference (solid symbols) are shown. The lines represent the biexponential fits to the data for the neat and the luciferase in the presence of Q4, but a monoexponential decay for the free FMN. The uncertainties are indicated by bars.

### 3.3. TRF measurements

In this study, time-resolved fluorescence intensity and anisotropy decays, i.e., $I(t)$ and $r(t)$, respectively, of FMN bound to luciferase and in solution (control) were collected in the frequency-domain (see Section 2.3). Figs. 3 and 4 show the representative data of $I(t)$ and $r(t)$, respectively, for the neat, the luciferase with Q4 and the free FMN samples. In both decays, the data of the free FMN were distinctively different from that of the luciferase with Q4 and the neat.

### 3.4. Fluorescence intensity decay analysis

A multiexponential decay model (Eq. (1)) was employed to fit the $I(t)$ data so as to assess the fluorescence quenching microenvironment of FMN in the enzyme and the effect of quinone in perturbing this microenvironment. Table 1 demonstrates the values of the resolved fluorescence intensity decay lifetime and intensity fraction, i.e., $\tau_i$ and $f_i$ (Eq. (3)), as well as the intensity-averaged lifetime, i.e., $\tau_{ave}$ (Eq. (4)), of FMN in the neat, the luciferase with Q4 and in the solution. Up to three decay components ($N=3$) were attempted to fit the data. For both the neat and the luciferase with Q4, the use of a decay function with $N=2$ (biexponential decay) represented a significant improvement in fitting the data over that with $N=1$ (monoexponential decay). This was clearly demonstrated by the two orders of magnitude decrease in the chisquare value as $N$ increased from 1 to 2 in both cases. On the contrary, the use of $N=3$ did not show any improvement as evident by the lack of a significant change in the chisquare value from $N=2$ to 3. In comparison, a monoexponential decay function fitted the data of the free FMN in solution sufficiently as the chisquare value remained similar for all values of $N$. The quality of the multiexponential decay fit to the frequency-domain data was also demonstrated in Fig. 3. Here the curves corresponding to $N=2$ for the neat and the luciferase with Q4, as well as those corresponding to $N=1$ for the free FMN clearly provided good fits to the data.

Fig. 5 shows the averaged fluorescence intensity decay parameters, $\tau_1$,$f_1$, $\tau_2$ and $\tau_{ave}$ based on the biexponential fit to the data collected from several independently prepared samples for the neat, the luciferase with quinone (Q1 to Q4) and the free FMN. The short decay lifetime $\tau_1$ was ~1 ns in the neat sample, but declined significantly to ~0.2–0.3 ns upon the addition of quinone. The longer decay lifetime $\tau_2$ was ~6 ns and the $\tau_{ave}$ ~4 ns in the neat. In the presence of quinone, the $\tau_2$ remained at ~4–6 ns and the $\tau_{ave}$ ~2–4 ns, independent of the order of the quinones. For the intensity fraction of the short decay component $f_1$, a peak value of ~0.6 was found for the Q2. These intensity decay parameters were compared with that of the free FMN in which a single decay lifetime of $\tau_1$ ~5 ns with $f_1=1$ were obtained.

It is important to mention that all the neat and the luciferase with quinone samples that we have studied exhibited biexponential decay behavior. This fluorescence intensity decay heterogeneity, i.e., the existence of discrete, and well-separated decay lifetimes, in each of those samples was further evaluated by a statistical parameter, chisquare ratio or $\chi^2_{1c}/\chi^2_{2c}$. This parameter is defined by the chisquare value of the monoexponential fit ($\chi^2_{1c}$) divided by that of the biexponential fit ($\chi^2_{2c}$). An improvement of the data fitting by the biexpeonential fit over the monoexponential fit should therefore result in a large chisquare ratio value (see Table 1). Fig. 5B shows the values of the chisquare ratio among all the samples. It is clear that this ratio was large, i.e., ~15–30, for the neat and the luciferase with quinone, but small, i.e., less than 2, for the free FMN (control).

### 3.5. Fluorescence anisotropy decay analysis

A multiexponential decay model (Eq. (2)) was employed to fit the $r(t)$ so as to assess the rotational mobility microenvironment of the

**Table 1**
Fluorescence intensity decay characteristics of the endogenous FMN in luciferase

| Sample | $\tau_1$ (ns) | $f_1$ | $\tau_2$ (ns) | $f_2$ | $\tau_3$ (ns) | $f_3$ | $\chi^2$ | $\tau_{ave}$ (ns) |
|---|---|---|---|---|---|---|---|---|
| Neat | 2.33 (0.02) | 1 | | | | | 112.87 | 2.33 (0.02) |
| | 0.97 (0.04) | 0.33 (0.01) | 5.61 (0.15) | 0.67 | | | 1.18 | 4.08 (0.12) |
| | 0.97 (0.04) | 0.34 (0.01) | 5.61 (0.15) | 0.65 (0.01) | 14.98 (1.05) | 0.01 | 1.34 | 4.13 (0.19) |
| Q4 | 1.81 (0.02) | 1 | | | | | 115.02 | 1.81 (0.02) |
| | 0.33 (0.05) | 0.22 (0.01) | 3.57 (0.09) | 0.78 | | | 4.65 | 2.86 (0.09) |
| | 0.01 (0.03) | 0.15 (0.20) | 2.35 (1.46) | 0.45 (0.10) | 4.78 (2.01) | 0.40 | 4.62 | 2.97 (1.70) |
| FMN | 4.91 (0.04) | 1 | | | | | 1.85 | 4.91 (0.04) |
| | 4.91 (0.12) | 0.99 (0.01) | 2.84 (1.01) | 0.01 | | | 2.07 | 4.89 (0.18) |
| | 0.01 (1.01) | 0.01 (0.01) | 4.91 (0.05) | 0.98 (0.01) | 22.65 (1.01) | 0.01 | 2.35 | 5.04 (0.12) |

The complex, heterogeneous decay behavior of the endogenous FMN in luciferase, in the absence (Neat) and presence of quinone Q4, is demonstrated by the multiexponential decay fits to the frequency-domain data (see Section 2.3). The recovered fluorescence decay parameters ($\tau_i$, $f_i$ and $\tau_{ave}$), their uncertainties (in parentheses) and chisquare values are shown. The data for the free FMN in solution (control) are also shown for comparison purpose.

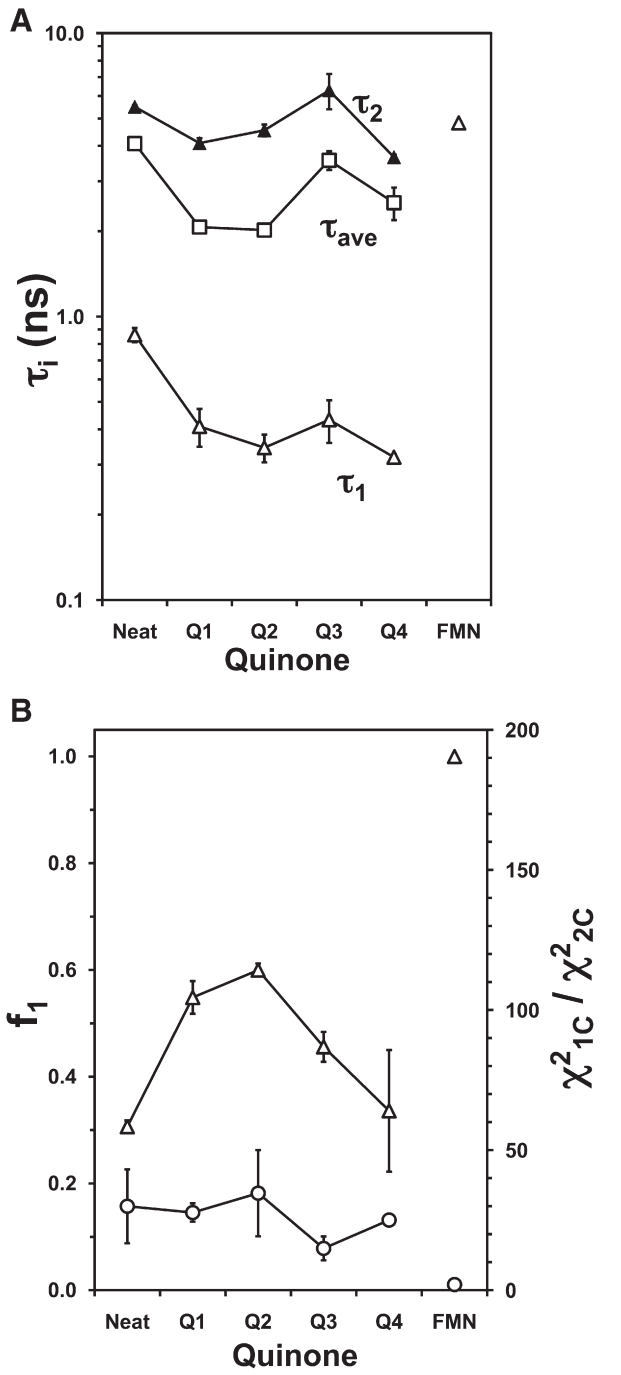


**Fig. 5.** Dependence of the fluorescence intensity decay parameters with quinone (Q1–Q4). Panel A shows the resolved decay lifetimes, short $\tau_1$ (open triangle) and long $\tau_2$ (solid triangle) and the intensity-average lifetime, $\tau_{ave}$ (open square). Panel B shows the intensity fraction of the short lifetime component $f_1$ (triangle) and the chisquare ratio (circle), chisquare value of the monoexponential fit $\chi^2_{1c}$ divided by that of the biexponential fit $\chi^2_{2c}$. Data from the neat, i.e., bound FMN in luciferase, and the free FMN in solution (control) are also shown.

FMN in the enzyme and the effect of quinone in perturbing this microenvironment. For the endogenous FMN with or without quinone, the anisotropy decay data were intrinsically nosier than the intensity decay data due to presence of the excitation and emission polarizers (see Section 2.3) that severely reduced the FMN fluorescence intensity, which was already rather low to start with. To improve the quality of the data fitting and suppress the uncertainties in the resolved decay parameters, the value of the initial anisotropy, i.e, $r_0$, was fixed to 0.40, the maximum possible value. Table 2 demonstrates the values of the resolved fluorescence anisotropy decay lifetime and molar fraction, i.e., $\phi_i$ and $\beta_i$. of FMN in the neat, the luciferase with Q4 and in the solution. Here, up to two decay components ($N=2$) were used to fit the data. The use of more than two decay components did not result in any significant improvement in the data fitting for all the samples we have studied, and in most cases it even failed to provide physically meaningful decay values, e.g., negative decay lifetimes or molar fraction greater than 0.4. For both the neat and the luciferase with Q4, the use of a biexponential decay function always resulted in a significant improvement in fitting the data over than the use of a monoexponential decay function. The was evident from the large decrease, i.e., ten or six times for the neat and the luciferase with Q4, respectively, in the chisquare values in these two samples as demonstrated in Table 2. In comparison, a monoexponential decay function fitted the data of the free FMN adequately as judged by the lack of any significant improvement or decrease in the chiquare value when a biexponential fit was used as shown in Table 2.

It is important to mention that our previous time-domain fluorescence decay measurements on FMN bound to luciferase suggest the presence of a long rotational decay lifetime, i.e., $\phi_2$, ~32 ns [10,22]. In those measurements, the value of $r_0$ was free in the data fitting instead of being fixed in this work. In this study, a smaller $\phi_2$, i.e., ~15 ns (Table 1), instead was observed. To test the significance of this long 32 ns-decay component, a biexponential fit but with $\phi_2$ fixed at 32 ns was also performed in all the samples. As demonstrated in Table 2, it is clear that the fixed $\phi_2$ improved the free two-component fit slightly for the neat sample, but not so for the luciferase with Q4 and the free FMN control.

Fig. 6 shows the averaged anisotropy decay parameters, $\phi_1$, $\beta_1$ and $\phi_2$ based on the biexponential fit to the data collected from several independently prepared samples for the neat, the luciferase with quinone and the free FMN. For comparison, the values of the first-order decay lifetime $\phi_p$ calculated from $r_{ss}$ and $\tau_{ave}$ (Eq. (5)) for all the samples are also shown. For the endogenous FMN in luciferase, the value of $\phi_1$ was ~0.2 ns for the neat and remained essentially unchanged in the presence of quinone. On the other hand, the value of $\phi_2$ was ~20–30 ns for the neat and the luciferase with Q1 or Q2. Yet, a sharp decline in the value of $\phi_2$ to ~6 or 4 ns was clearly observed when Q3 or Q4 was added, respectively. Note that a steady decline in the value of $\phi_p$ from ~3 to 1 ns following the order of quinone was observed. The above anisotropy decay parameters of endogenous FMN were compared with that of the free FMN in which a single anisotropy decay lifetime, i.e., $\phi_1$ or $\phi_p$ ~0.04 ns, was observed.

The averaged values of $\beta_1$ for all the samples, as well as the chisquare ratio (see Section 3.4), for the samples are presented in Fig. 6B. Here a progressive increase in the value of $\beta_1$ from ~0.20 (neat) to ~0.32 (luciferase with Q4) was found. This corresponds to an increase of the mole% of the short decay component from ~50 to 80%. Interestingly, the chisquare ratio was between 5 and 10 for the neat and the luciferase with

**Table 2**
Fluorescence anisotropy decay characteristics of the endogenous FMN in luciferase

| Sample | $\phi_1$ (ns) | $\beta_1$ | $\phi_2$ (ns) | $\beta_2$ | $\chi^2$ |
|---|---|---|---|---|---|
| Neat | 1.722 (0.016) | 0.40[f] | | | 126.00 |
| | 0.130 (0.040) | 0.194 (0.055) | 15.07 (3.56) | 0.206 | 15.06 |
| | 0.277 (0.020) | 0.240 (0.014) | 32[f] | 0.160 | 7.30 |
| Q4 | 0.374 (0.027) | 0.40[f] | | | 12.20 |
| | 0.144 (0.070) | 0.311 (0.007) | 4.64 (0.51) | 0.089 | 2.93 |
| | 0.149 (0.014) | 0.288 (0.019) | 32[f] | 0.112 | 10.39 |
| FMN | 0.113 (0.005) | 0.40[f] | | | 5.12 |
| | 0.128 (0.004) | 0.404 (0.004) | 187 (2766) | −0.004 | 5.14 |
| | 0.080 (0.039) | 0.645 (0.311) | 32[f] | −0.245 | 15.73 |

The complex, heterogeneous anisotropy decay behavior of the endogeneous FMN in luciferase, in the absence (Neat) and presence of quinone Q4, is demonstrated by the multiexponential decay fits to the frequency-domain data (see Section 2.3). The recovered decay parameters ($\phi_i$ and $\beta_i$), their uncertainties (in parentheses) and chisquare values are shown. The data for the free FMN in solution (control) are also shown for comparison.

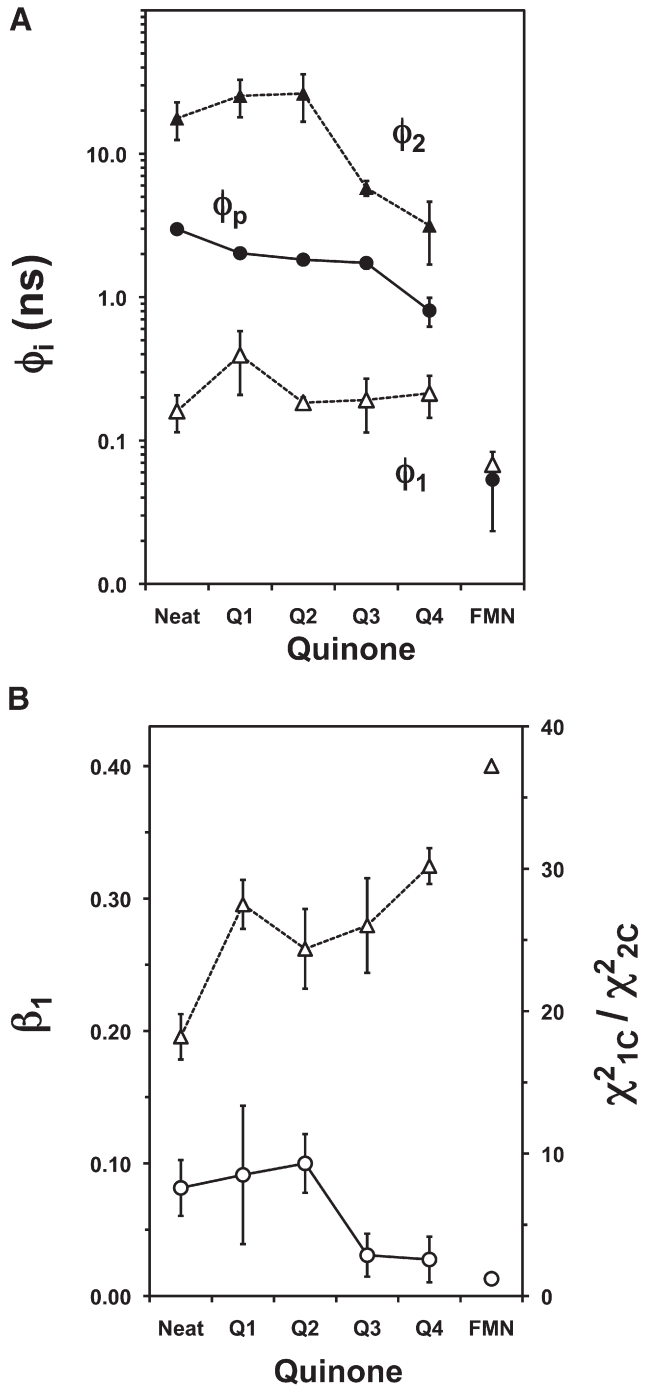


**Fig. 6.** Dependence of the fluorescence anisotroy decay parameters with quinone (Q1–Q4). Panel A shows the resolved anisotropy decay lifetimes, short $\phi_1$ (open triangle) and long $\phi_2$ (solid triangle). The anisotropy decay lifetime $\phi_p$ (solid circle) determined by the Perrin model (Eq. (5)) is also shown. Panel B shows the fraction of the short lifetime component $\beta_1$ (triangle) and the chisquare ratio (circle). See the legend of Fig. 5 for more details.

Q1 or Q2, but abruptly dropped to ~2. In comparison, the value of $\beta_1$ was 0.4 and the chisquare ~1 for the free FMN in solution.

## 4. Discussion

Endogenous FMN bound to bacterial luciferase represents an intrinsic, noninvasive fluorophore to probe the conformational dynamics and FMN/protein interactions at the FMN binding region, or active site, of the enzyme. In addition, it also provides useful information about the effect of quinone, a known inhibitor of the bacterial bioluminescence process, on those conformation and interactions that are further associated with the enzyme inhibition mechanism of quinone. We have investigated the effects of quinones of different levels of hydrophobicity on the quenching and mobility of the endogenous FMN based on the fluorescence intensity and rotational decay dynamics of this bound FMN.

### 4.1. Fluorescence intensity decay heterogeneity of endogenous FMN

The presence of two discrete and well-separated intensity decay lifetimes, $\tau_1$ of ~1 ns with $f_1$ of ~30% and $\tau_2$ of ~4 ns, or intensity decay heterogeneity, of the neat sample suggests that the endogenous FMN senses a heterogeneous fluorescence quenching microenvironment at the active site of the luciferase. This is what one would expect for a substrate molecule, like FMN, bound to a site-specific region of an enzyme [10,22]. The quenching microenvironment of endogenous FMN is strongly influenced by the conformational dynamics of the amino-acid residues surrounding the FMN at the active site. As expected, our control, the free FMN in solution (isotropic environment), exhibited a single decay lifetime ~5 ns, i.e., no intensity decay heterogeneity.

Interestingly, this intensity decay heterogeneity of endogenous FMN was largely preserved in the presence of quinone. The rather large chisquare ratio value of the endogenous FMN (with or without quinone) versus the small chisquare ratio value of the free FMN (Fig. 5B) justifies the statistical significance of the intensity decay heterogeneity. However, neither the resolved decay lifetime nor the intensity fraction (Fig. 5) correlates with the LogP value of the quinone (Fig. 2B). These findings indicate that the subtle change in the conformational dynamics of the enzyme at the active site bears no direct relationship with the hydrophobicity of the added quinone. Perhaps, the change is related to the specific chemical structure of each quinone. Since the interaction of quinone with luciferase is non-specific and involves many possible sites, no conclusion can be drawn at this time to correlate the structure of quinone with the quenching property of endogenous FMN based on the TRF results alone.

### 4.2. Fluorescence anisotropy decay heterogeneity of endogenous FMN

The presence of two largely separated anisotropy decay lifetimes, $\phi_1$ of ~0.2 ns with $\beta_1$ of ~0.2 and $\phi_2$ of ~20 ns, or anisotropy decay heterogeneity, of the neat sample reveals that the endogenous FMN probes a rotationally heterogeneous microenvironment at the active site of the luciferase. The rotational mobility of the endogenous FMN is strongly influenced by the FMN/protein interactions, or binding affinity of FMN, at the active site of the enzyme. The existence of two anisotropy decay lifetimes may indicate the existence of two FMN binding sites, weak and strong, which are associated with the fast $\phi_1$ and slow $\phi_2$ components, respectively. The fast component is not associated with the unbound FMN, or free FMN, since the latter has a much shorter decay lifetime of $\phi_1$ ~0.04 ns as revealed from our control (Fig. 6A).

A subtle response of the resolved anisotropy decay parameters to quinone was found. Here, the short decay lifetime $\phi_1$ remained insensitive to quinone, but a large decline in the long decay lifetime $\phi_2$ in response to Q3 or Q4 was observed. Note that a progressive increase in $\beta_1$ following the order of Q1 to Q4, or the level of hydrophobicity of quinone, was evident (Fig. 6A). These results indicate that the endogenous FMN senses a more rotationally flexible environment in the presence of the most hydrophobic quinones, Q4 and Q5. Also, the fraction of the more flexible, or faster rotating component $\beta_1$ increases with the increasing hydrophobicity of the added quinone and approaches the maximum value of 0.40, or the value for the free FMN in solution. Also, the average rotational rate of the endogenous FMN, which is inversely proportional to the value of $\phi_p$ [28,32], also

increases progressively with the increasing hydrophobicity of the added quinone, and, therefore, further supports the above trend. Interestingly, the lower chisquare ratio values for the luciferase with Q4 and Q5 further indicate that the anisotropy decay heterogeneity of the endogenous FMN is diminished in the presence of those highly hydrophobic quinones.

### 4.3. Implication of the enzyme inhibition mechanism of quinone

As discussed in Section 4.2 above, the averaged rotational rate and the fraction of the faster rotating component increase with the hydrophobicity of the quinone. Based on these findings, we propose that the added quinone reduces the averaged binding affinity of the endogenous FMN to the active site of luciferase by increasing the fraction of the weak FMN binding sites of luciferase. The mechanism may be associated with the competition between the added quinones and the larger FMN substrate in their interactions with the amino acid residues at the active site of luciferase, especially those involving the hydrophobic interaction. Also, the perturbation of the secondary or tertiary structure of luciferase by quinones at various locations of the enzyme, including those not associated with the binding region of FMN, may be involved. The latter is classified as the non-specific interactions of quinone with the enzyme.

Lastly, a previous work [33] on the effect of the same homologous quinones on the inhibition of a bioluminescence reaction of bacterial luciferase has been performed. In that work, a correlation between the level of inhibition by quinone and the hydrophobicity of the quinone was also established. Therefore, a link between the hydrophobicity of the small organic molecules and the inactivation of the enzyme via the perturbation of the rotational flexibility of the substrate (FMN in our case) of the enzyme can be established. Whether a similar mechanism operates on other inhibitor/enzyme systems awaits further investigations.

## Acknowledgement

The work was supported by grants from Welch Research Foundation (D-1158); US National Institutes of Health (CA47610); Russian Federal Agency of Science and Innovation (02.444.11.7304); the Program "Molecular and Cellular Biology" and “Leading Scientific School” of the Russian Academy of Sciences.

## References

[1] E. Fedorova, N. Kudryasheva, A. Kuznetsov, O. Mogil'naya, D. Stom, Bioluminescent monitoring of detoxification processes: activity of humic substances in quinone solutions, J. Photochem. Photobiol. B 88 (2007) 131–136.
[2] S. Girotti, E.N. Ferri, M.G. Fumo, E. Maiolini, Monitoring of environmental pollutants by bioluminescent bacteria, Anal. Chim. Acta 608 (2008) 2–29.
[3] A. Roda, P. Pasini, M. Mirasoli, E. Michelini, M. Guardigli, Biotechnological applications of bioluminescence and chemiluminescence, Trends Biotechnol. 22 (2004) 295–303.
[4] T.V. Rozhko, N.S. Kudryasheva, A.M. Kuznetsov, G.A. Vydryakova, L.G. Bondareva, A.Y. Bolsunovsky, Effect of low-level alpha-radiation on bioluminescent assay systems of various complexity, Photochem. Photobiol. Sci. 6 (2007) 67–70.
[5] O. Tchaikovskaya, I. Sokolova, V. Svetlichnyi, E. Karetnikova, E. Fedorova, N. Kudryasheva, Fluorescence and bioluminescence analysis of sequential UV-biological degradation of p-cresol in water, Luminescence 22 (2007) 29–34.
[6] E. Vetrova, E. Esimbekova, N. Remmel, S. Kotova, N. Beloskov, V. Kratasyuk, I. Gitelson, A bioluminescent signal system: detection of chemical toxicants in water, Luminescence 22 (2007) 206–214.
[7] N.S. Kudryasheva, Bioluminescence and exogenous compounds: physico-chemical basis for bioluminescent assay, J. Photochem. Photobiol. B 83 (2006) 77–86.
[8] N. Kudryasheva, E. Vetrova, A. Kuznetsov, V. Kratasyuk, D. Stom, Bioluminescence assays: effects of quinones and phenols, Ecotoxicol. Environ. Saf. 53 (2002) 221–225.
[9] R.J. Mitchell, M.B. Gu, An *Escherichia coli* biosensor capable of detecting both genotoxic and oxidative damage, Appl. Microbiol. Biotechnol. 64 (2004) 46–52.
[10] E.V. Vetrova, N.S. Kudryasheva, V.A. Kratasyuk, Redox compounds influence on the NAD(P)H:FMN-oxidoreductase-luciferase bioluminescent system, Photochem. Photobiol. Sci. 6 (2007) 35–40.
[11] T. Wilson, J.W. Hastings, Bioluminescence, Annu. Rev. Cell Dev. Biol. 14 (1998) 197–230.
[12] J.W. Hastings, J.G. Morin, Photons for reporting molecular events: green fluorescent protein and four luciferase systems, Methods Biochem. Anal. 47 (2006) 15–38.
[13] F. McCapra, Chemical generation of excited states: the basis of chemiluminescence and bioluminescence, Methods Enzymol. 305 (2000) 3–47.
[14] E.V. Nemtseva, N. Kudryasheva, The mechanism of electronic excitation in the bacterial bioluminescent reaction, Russ. Chem. Rev. 76 (2007) 91–100.
[15] A.J. Fisher, F.M. Raushel, T.O. Baldwin, I. Rayment, Three-dimensional structure of bacterial luciferase from *Vibrio harveyi* at 2.4 A resolution, Biochemistry 34 (1995) 6581–6586.
[16] Z. Li, R. Szittner, E.A. Meighen, Subunit interactions and the role of the luxA polypeptide in controlling thermal stability and catalytic properties in recombinant luciferase hybrids, Biochim. Biophys. Acta 1158 (1993) 137–145.
[17] J. Vervoort, F. Muller, D.J. O'Kane, J. Lee, A. Bacher, Bacterial luciferase: a carbon-13, nitrogen-15, and phosphorus-31 nuclear magnetic resonance investigation, Biochemistry 25 (1986) 8067–8075.
[18] T. Sandalova, Y. Lindqvist, Three-dimensional model of the alpha-subunit of bacterial luciferase, Proteins 23 (1995) 241–255.
[19] H.R. Leenders, J. Vervoort, A. van Hoek, A.J. Visser, Time-resolved fluorescence studies of flavodoxin. Fluorescence decay and fluorescence anisotropy decay of tryptophan in Desulfovibrio flavodoxins, Eur. Biophys. J. 18 (1990) 43–55.
[20] R. Leenders, M. Kooijman, A. van Hoek, C. Veeger, A.J. Visser, Flavin dynamics in reduced flavodoxins. A time-resolved polarized fluorescence study, Eur. J. Biochem. 211 (1993) 37–45.
[21] R. Leenders, A. Van Hoek, M. Van Iersel, C. Veeger, A.J. Visser, Flavin dynamics in oxidized *Clostridium beijerinckii* flavodoxin as assessed by time-resolved polarized fluorescence, Eur. J. Biochem. 218 (1993) 977–984.
[22] E.V. Vetrova, N.S. Kudryasheva, A.J. Visser, A. van Hoek, Characteristics of endogenous flavin fluorescence of *Photobacterium leiognathi* luciferase and *Vibrio fischeri* NAD(P)H:FMN-oxidoreductase, Luminescence 20 (2005) 205–209.
[23] A.M. Kuznetsov, N.A. Tyulkova, V.A. Kratasyuk, V.V. Abakumova, E.K. Rodicheva, A study of the properties of reagents for bioluminescent bioassays, Sib. Ekol. Z. 5 (1997) 459-206.
[24] J.R. Lakowicz, B.P. Maliwal, Construction and performance of a variable-frequency phase-modulation fluorometer, Biophys. Chem. 21 (1985) 61–78.
[25] E. Gratton, D.M. Jameson, R.D. Hall, Multifrequency phase and modulation fluorometry, Annu. Rev. Biophys. Bioeng. 13 (1984) 105–124.
[26] B. Cannon, A. Lewis, J. Metze, V. Thiagarajan, M.W. Vaughn, P. Somerharju, J. Virtanen, J. Huang, K.H. Cheng, Cholesterol supports headgroup superlattice domain formation in fluid phospholipid/cholesterol bilayers, J. Phys. Chem. B 110 (2006) 6339–6350.
[27] R.D. Spencer, G. Weber, Influence of Brownian rotation and energy transfer upon the measurements of fluorescence lifetime. J. Chem. Phys. 52 (1970) 1654–1663.
[28] K.H. Cheng, J. Virtanen, P. Somerharju, Fluorescence studies of dehydroergosterol in phosphatidylethanolamine/phosphatidylcholine bilayers, Biophys. J. 77 (1999) 3108–3119.
[29] K.H. Cheng, Fluorescence depolarization study of lamellar liquid crystalline to inverted cylindrical micellar phase transition of phosphatidylethanolamine, Biophys. J. 55 (1989) 1025–1031.
[30] B. Cannon, G. Heath, J. Huang, P. Somerharju, J.A. Virtanen, K.H. Cheng, Time-resolved fluorescence and fourier transform infrared spectroscopic investigations of lateral packing defects and superlattice domains in compositionally uniform cholesterol/phosphatidylcholine bilayers, Biophys. J. 84 (2003) 3777–3791.
[31] PubChem. NCBI (http://pubchem.ncbi.nlm.nih.gov).
[32] F. Perrin, Mouvement brownien d'un ellipsoide. II. Rotation libre et dipolarisation des florescences. Transaction et diffusion de molecules ellipsoidoles. J. Phys. Radium. 71 (1936) 1–44.
[33] N. Kudryasheva, Ph.D. Thesis, Institute of Biophysics, Siberian Branch of the Russian Academy of Sciences (1991).